Contributions to the UBC Quantum Degenerate Gas Lab:

By: Paul Lebel
APSC 110

Supervisor: Dr. Kirk Madison
Date Submitted: 09/05/2005

2757-1 Fairview Crescent
Vancouver, BC
V6T 2B9

May 3rd, 2005

Dr. Kirk Madison
Professor of Physics
Department of Physics and Astronomy
6224 Agricultural Road
Vancouver, B.C. V6T 1Z1

Dear Dr. Madison:

Subject: Coop report for work completed January-April 2005

In response to the Science Coop office's request for a formal work term report and for future reference within the lab, I present to you my work term report titled "Contributions to the UBC Quantum Degenerate Gas Lab: January-April 2005".

This report describes the development of magnetic trapping coils and other small projects completed by me during the term, but also covers some background theory including a short, classical description of the Magneto-Optical Trap. The coil construction details and some testing of the coil prototype are included within the coil section.

It was a joy to work with you and the others in the lab this term and also to write this report. I am sure it will meet your approval.

Sincerely,

Paul Lebel

Enclosure

Contributions to the UBC Quantum Degenerate Gas Lab:

January-April 2005

Prepared for:
Dr. Kirk Madison
Department of Physics and Astronomy
University of British Columbia

By: Paul Lebel
2nd Year Engineering Physics
University of British Columbia
Date Submitted: 09/05/2005

Preface

The majority of this report focuses on the work I completed by during my first cooperative work placement, in the second year of engineering physics at UBC. The goal is to present the work completed as being a part of a much larger, complex experiment worked on by professors, graduate students, and other undergraduates. As such it would be impossible to attempt a complete description of the lab; however a significant section is devoted to both the Magneto-Optical Trap and the goals of the UBC Quantum Degenerate Gas lab in order to create some perspective for my contributions over the term.

From reading other papers on atom cooling and trapping, I have noticed that these experiments are characterized by having as much equipment as possible packed onto optics tables and their immediate proximity. This goes to show how much it takes to achieve temperatures cold enough to study low temperature physics and the ensuing quantum mechanical effects. However, it is a brand new field and it relates to a broad range of new technologies currently in conception, so current interest in atom cooling and trapping is essentially exploding (so most publications remark) and you can be sure to expect lots of breakthroughs in the near future.

Although the lab is still in its developing stages, I can see it growing rapidly in the direction of achieving its goals thanks to all the very intelligent and hard working people there. My only regret is having to leave after only 4 months, to return to regular classes. My thanks to Bruce, Tao, Swati, Ray, Amy, Janelle, and of course Kirk Madison for a great 4 months!

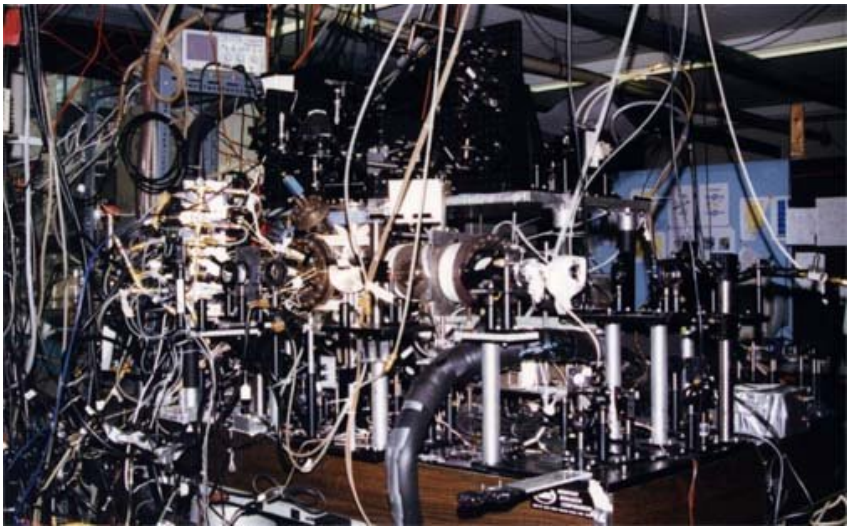

Figure 1: A BEC experiment at MIT

ABSTRACT

In this report, various tasks around the UBC Quantum Degenerate Gas lab are described. Included is a classical description of the Magneto-Optical Trap, intended as motivation/contextual support for the work completed. In the current term a pair of custom, multipurpose, water cooled, magnetostatic trapping coils has been designed. The coils are suitable for use in a Magneto-Optical Trap as well as for magnetic trapping and the studying of feshbach resonances. They are custom sized for a hand-blown quartz UHV chamber, but not restricted to use on that specific chamber. A prototype coil was constructed and partially tested. Other projects include photolithographic etching, machine shop work, and response analysis of the master laser diode to several stimuli.

TABLE OF CONTENTS

LIST OF FIGURES

GLOSSARY OF TERMS

BEC	Bose-Einstein Condensate. A degenerate state of matter predicted to exist by Albert Einstein and Satyendra Bose.
GUI	Graphical User Interface
Magneto-Optical Trap (MOT)	Atom trapping technique pioneered in 1987 by AT&T Bell Labs.
PID Controller	Controller using proportional, integral, and differential feedback components to output a programmable and stable value.
Piezoelectric Crystal	A crystal with the peculiar but very useful property of a physical expansion or contraction resulting from an applied voltage. Used to distort the shape of the laser cavity; for frequency modulation.
PVC	Polyvinylchloride plastic used for the coil housings
Saturated Absorption	With two counter-propagating laser beams (split from the same source) shining through a vapor cell, atoms with nearly zero velocity will absorb photons from either beam with equal probability. If one beam is weaker, it will see a decrease in absorption from those atoms of near zero velocity because they have already been excited by the stronger beam.
TOP Trap	Time Orbiting Potential Trap. Uses AC currents in trapping coils to shift the zero point of a magnetic trap around in a circular pattern so the atoms cannot ever reach it.

1.0 BACKGROUND AND INTRODUCTION

The UBC Quantum Degenerate Gas lab (QDG), led by Dr. Kirk Madison, is among several groups around the world exploring the new and exciting field of atom trapping and cooling. In general, the objective is to obtain samples of matter which are both cold enough and dense enough such that de Broglie wavelengths overlap and the behavior of the system is dominated by quantum effects. The phase space density, ρ, characterizes the degree to which this is true. Values of ρ on the order of unity must be achieved before classical physics breaks down (For a typical room temperature gas, ρ is on the order of 10^-6) [3]

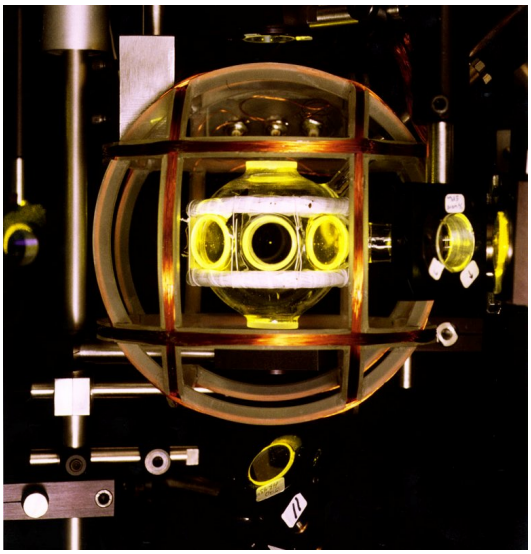

Figure 2: The Magneto-Optical Trap built by Dr. Kirk Madison in 1998

$$\rho = n\lambda_{db}^3 \qquad \lambda_{db} = \frac{h}{\sqrt{3mkT}}$$

Where λ_{db} is the de Broglie wavelength, n is the number density, h is Planck's constant, m is the mass, k is Boltzmann's constant, and T is temperature in Kelvin. Back in 1924, Satyendra Bose and Albert Einstein predicted the existence of a new phase of matter which will only form when a macroscopic number of atoms are all in the lowest possible energy state: the zero momentum state. It is called a Bose Einstein Condensate (BEC), and is characterized by a dense lump of matter in the trap center. BEC was considered to be one of the holy grails in physics[3] since the time of its prediction, and was finally achieved by Cornell and Wieman in 1995. Such experiments help to unravel many modern mysteries in physics, including but not limited to:

- High Temperature Superconductivity
- Means of establishing Q-bits for quantum information processing
- Atom lasers
- De Broglie interferometry

Obtaining ultra cold atoms is by no means trivial. In order to prevent contact with ambient temperature atoms/molecules, trapping and cooling must be implemented by means such as radiation pressure and magnetic confinement, where there is no direct physical contact between the sample and its high-energy surroundings.

The concept of cooling by radiation pressure has been suggested over 50 years ago[1], however it is relatively recent advances in optical technology that have allowed researchers to gain the elegant manipulation of light necessary to control atom-light interactions to a meaningful extent. Lasers are of course the life-giving technology necessary for nearly any experiment in atom trapping and cooling. This is because for an atom to absorb a photon (and therefore its momentum), that photon's energy must be very close to one of the electronic energy level transitions predicted by quantum mechanics. Any regular light source has a very wide distribution of frequencies and offers little control over which atoms will be affected and which energy transitions will occur. Lasers allow very precise control over the frequency, intensity, beam shape, propagation angle, phase, and polarization of the light interacting with a cloud of atoms and can be used to guide them into a trap by choosing a specific transition and tuning the laser to excite it (although still only in a statistical fashion). The first real atom traps were demonstrated in 1985 by AT&T Bell labs: one showing beam slowing (cooling) and the other magnetic trapping[1]. Two years later, both trapping and cooling were achieved in what is called a Magneto-Optical Trap (MOT). The MOT has since become a robust and relatively easy method of trapping and cooling atoms; it can produce temperatures on the order of 10^{-5}K and densities of order 10^{10} cm^{-3}, leading to a phase space density of order 10^{-6}. It is generally used as a first stage in cooling atoms to nano-Kelvin temperatures and will be described in its self-titled section below.

After trapped in a MOT, atoms may be transferred into one of several types of magnetic traps to be further cooled by a process called evaporative cooling. During evaporative cooling, atoms in higher energy states are selectively removed from the trap by lowering the confining potential, thereby reducing the average energy of the cloud.

1.1 The Magneto-Optical Trap

The general concept of how a MOT accomplishes cooling and trapping is fairly straightforward and can be described by a damped harmonic motion model. A cloud of atoms in a MOT is analogous to a mass on a spring, i.e. there is both a position dependant force (the spring force) and a velocity dependant force (the damping force). Together these forces produce both cooling and trapping of atoms in a vacuum cell. Although the forces of radiation pressure in a MOT are more complex than this, the average forces on a cloud can be treated as such because the cloud in a MOT is neither cold nor dense enough to be dominated by the quantum regime ($\rho << 1$).

The cooling and trapping forces are produced by six counter-propagating laser beams

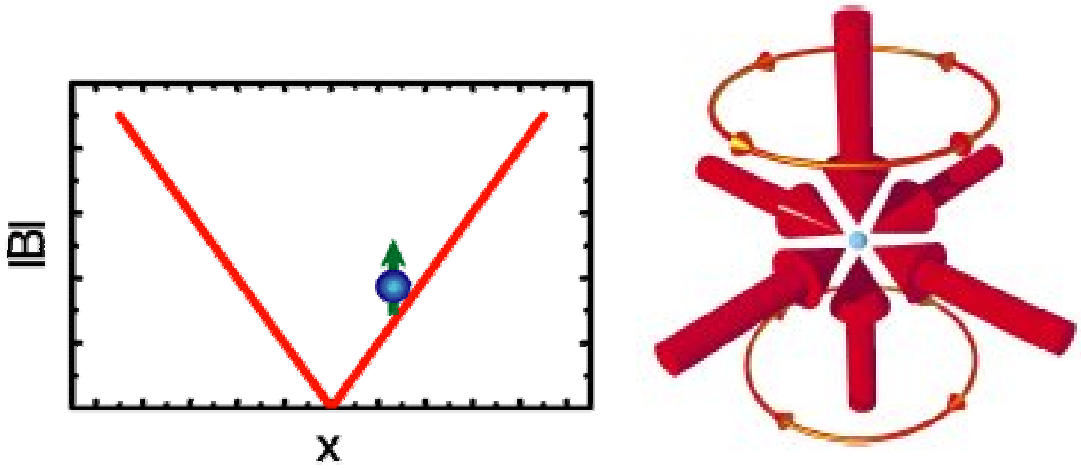

Figure 3: (left) Qualitative plot of the magnetic field intensity along one axis passing through the trap center. (right) The six counter-propagating laser beams and the opposing current loops of a MOT.

combined with an inhomogeneous magnetic field. The lasers arrive from each axis in a Cartesian 3-space, i.e. from the six faces of a cube (the atoms being in the center of the cube). Every photon carries momentum $p = \frac{\hbar \varpi}{c}$ which in principle may be transferred to an atom when absorbed. If the lasers' frequency ϖ was tuned directly to the desired energy transition, the trap would not work because the atoms would see an equal force from all sides and neither trapping nor cooling would be achieved.

The lasers are therefore detuned below the chosen energy transition so that an atom moving

away from the trap in the $+Z$ direction will see the -Z beam to be Doppler shifted by an amount $\delta = \vec{k} \cdot \vec{v}$, while it sees the $+Z$ beam shifted by $\delta = -\vec{k} \cdot \vec{v}$. Assuming δ has the correct sign, the atom is more likely to absorb the beam which decelerates it, and less likely to absorb the beam which accelerates it.

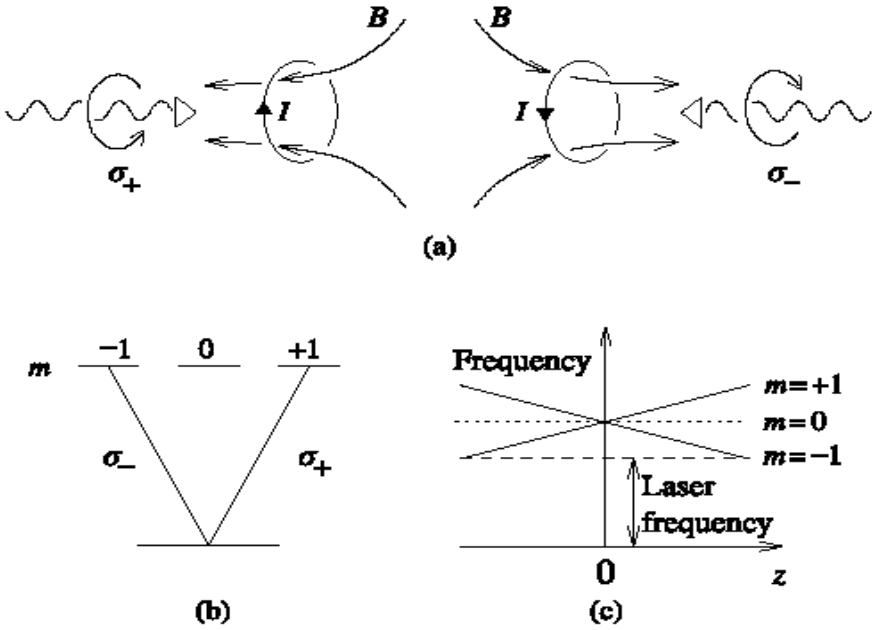

Figure 4 [4]: Influence of the quadrupole magnetic field on a two-level atom. (a) Current loops and field direction are shown. Atoms on the left see a RHCP beam as σ_+, and atoms on the right see a RHCP beam as σ_-. The changing B field causes this discrepancy. (b) Induced transitions from the opposing beams: σ_- light can excite to the *Ms = -1* state and σ_+ light may excite to the *Ms = +1* state. (c) Zeeman splitting in a linear magnetic field gradient.

The second force, the spring-like restoring force, occurs as a result of the laser detuning in the presence of a magnetic field gradient. The magnetic field is zero at the center of the trap and for small distances it increases linearly as a function of distance from the trap center. Opposing sides of the trap also have opposing field direction. As shown in figure 4[4], the splitting of the $M_s = -1$ sublevel on one side of the trap is positive, whereas on the other side it is negative, and visa-versa for $M_s = +1$. Since the hyperfine energy splits are due to the projection of angular momentum onto the magnetic field axis, allowed transitions are restricted by the projection of the light's polarization axis on the magnetic field. This means if both beams are RHCP with respect to direction of propagation and the atom is at a

non-zero field location, only one beam can induce a transition to the *Ms = -1* (the σ_- beam), while the other can only induce a transition to the *Ms = +1* (the σ_+ beam). The atom's position will dictate which one of these states will be preferentially excited, and only one of the counter-propagating beams is able to do so. In the words of Raab et al from AT&T Bell Labs[1], the trap exploits the atom's internal structure to induce a greater absorption probability for light moving toward the center of confinement.

1.1.1. Damped Harmonic Motion

The spring force can be approximated by a linear function

$$F_s = -\kappa z = -\frac{dB}{dz}\gamma z$$

where γ is a constant on the order of 10^{-11} N/G. The damping force may also be approximated as being linearly dependant on velocity

$$F_v = -\alpha v$$

where α is a constant on the order of 10^{-13} $\frac{N}{cm/s}$. The differential equation describing the motion of the atoms is then

$$mz'' + \alpha z' + \kappa z = 0$$

Assuming they are not driven by another force, the atoms will oscillate at a frequency

$$\omega_o = \sqrt{\frac{\kappa}{m}}$$

If the magnetic field gradient is 30 *G/cm*, then

$$\omega_o = \sqrt{\frac{\kappa}{m}} = \sqrt{\frac{30*10^{-21}}{38*10^{-27}}} = 890 s^{-1}$$

and the damping time constant $\tau = \frac{\alpha m}{\kappa^2} = 4ms$. Note the motion does not follow this model as the speeds become small because the atoms' velocity is too small to adequately Doppler shift the incoming light. This is called the Doppler limit. Further cooling in a MOT is possible through other mechanisms such as Sisyphus cooling, which shall not be discussed here.

1.1.2. Laser Locking and Saturated Absorption

The Master Laser alone does not produce a stable and accurate beam that is sufficiently near the correct absorption frequency needed for the MOT—it must be actively locked by a somewhat involved method using a saturated absorption cell. A glass cell containing ^{87}Rb atoms is placed in the path of the beam, and the atoms attenuate a small bandwidth of order 5 MHz centered about the correct energy transition, plus approximately a 2 GHz bandwidth caused by the Maxwell-Boltzmann distribution of velocities found in the cell. To overcome the Doppler Broadening, two counter-propagating beams are used: one a 'probe' beam and one a 'pump' beam. A moving atom will see the beams Doppler shifted in opposite directions and therefore will more likely absorb one over the other. A stationary atom, on the other hand, is equally likely to absorb a photon from either direction assuming there are equal numbers of each. The pump beam is purposely made more intense and serves to excite to saturation the atoms having close to zero velocity. The probe beam therefore sees a distinct drop in absorption for only those very slow moving atoms. This fact is used to distinguish the atoms' absorption peak and is sent to electronics in the lock box. The lock box sends signals to the Proportional Integral Differential current controller and piezoelectric crystals, which actively modulate the laser current (and frequency).

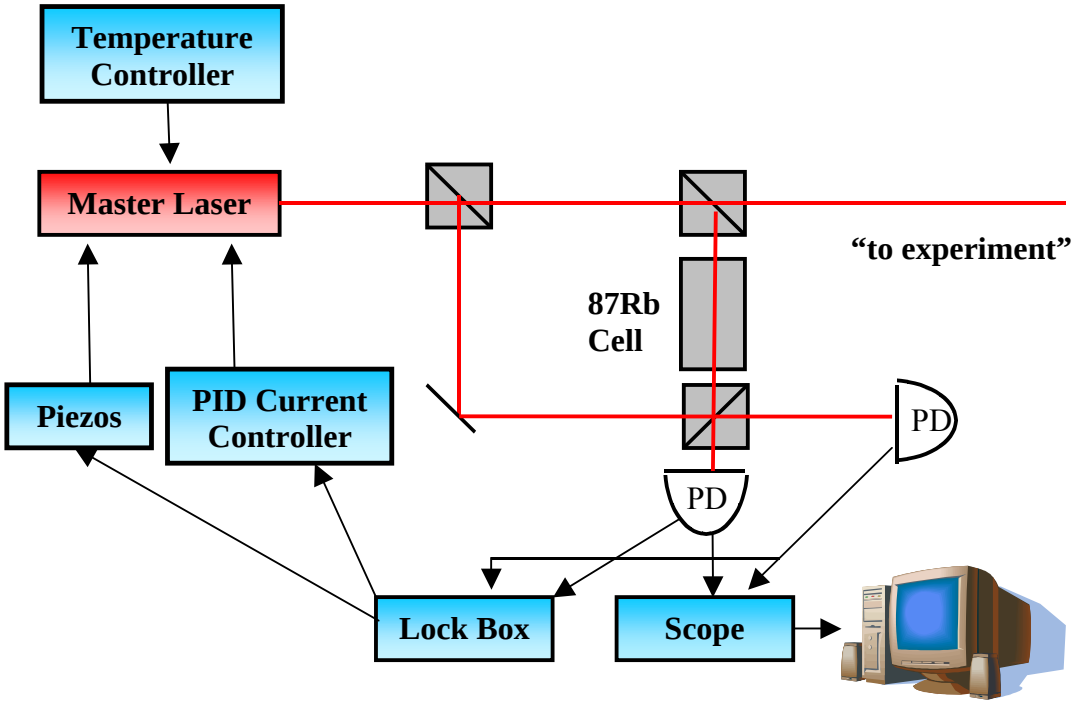

Figure 5: Schematic of the laser-locking process. A portion of the master laser shines through a 87Rb saturated absorption cell and the correct frequency is identified and locked.

1.1.3 Other Considerations

Ultra High Vacuum: Collisions with room temperature atoms are disastrous to a MOT and must be kept to a minimum. For this reason UHV conditions are kept in the MOT cell where the atoms are trapped. Pressures of 10^{-11} were maintained in the very first MOT experiment in 1987. All parts must be baked in a high temperature oven before use in a UHV system.

Temperature Fluctuations: Changing temperatures cause most materials to expand and contract. Excellent temperature control is needed in the lab to prevent anything from changing size during the experiment. For example, the master laser cavity can change length with a temperature change and lase at the wrong frequency.

Sound/Mechanical Vibrations: Lasers respond to mechanical waves. Even small noises or taps on the optics table can induce a mode hop in the laser, jumping it out of range for the experiment.

Background radiation: Any electro-magnetic radiation from outside sources can affect the experiment. Electronics parts can act as antennas and become influenced by this outside noise.

1.2 Current Progress of the QDG Lab

As an initial step towards achieving ultra-cold atoms, the lab is currently working on establishing a functional lithium and rubidium MOT. The necessary modules are:

- Ultra High Vacuum system (UHV)
- Custom blown glass vacuum cell with optical access windows
- Saturated absorption-locked master laser diode
- Slave lasers
- Quadrupole magnetic field gradient produced by an anti-Helmholtz coil configuration
- Sources of Lithium and Rubidium atoms accessible to the UHV system
- Computer control system

The lab boasts three full size optical tables on which the experiments will be set up. The middle table contains one master laser diode already in operation, with the saturated absorption locking mechanism currently undergoing testing. Slave lasers are to be set up on the far optics table this summer of 2005 by fourth year UBC engineering physics

students Aviv Keshet and Peter Eugster. The quadrupole magnetic field gradient is to be produced by the multi-purpose trapping coils designed and tested by the author during the current term, January-April 2005. The glass cell is a tried and true custom quartz crystal cell used by Dr. Madison during his PhD thesis at the University of Austin in Texas.

UHV conditions are to be supplied by a Varian Vacuum turbo V-70 pump station. Maintaining these conditions requires considerable precautions when installing any part which comes in contact with the vacuum system. All parts must be baked in a high-temperature oven to burn off any vapor-producing contaminants, and subsequently handled with care.

Inserted into the lower arm of the quartz cell will be a ^{6}Li dispenser designed by Swati Singh, a graduate student working in the lab. Commercially available Li dispensers contain 7% ^{6}Li and 93% ^{7}Li, as compared to the pure ^{6}Li which is desired for the experiment. Also present in the UHV system will be a commercially made ^{87}Rb dispenser.

To coordinate the multitude of devices all working simultaneously to run the MOT, a computer control system based on that used by Meyrath et al. in Texas is also currently under development by Raymond Gao, a 2nd year physics and computer science undergraduate.

1.3 Future Goals of the QDG Lab

After establishing a Magneto-Optical Trap, the QDG lab will build a magnetic trap to study collisional interactions and eventually produce a BEC. As mentioned in the introduction, magnetic traps use evaporative cooling to lower the average energy of atoms. The effectiveness of evaporative cooling depends strongly on collisional interactions between atoms in the cloud. It is desirable for a sample to undergo many elastic collisions in a short amount of time, and these can be maximized by tuning an external magnetic field to induce a feshbach resonance.

2.0 MULTI-PURPOSE TRAPPING COILS

A pair of multi-purpose, water cooled atom trapping coils has been designed for use in a MOT and a magnetic trap. Although the current work term did not allow time to construct the coils, a complete prototype was built and tested, from which results are displayed in section 2.5.

Thanks to switching electronics and current controllers, one pair of coils can be used for several functions. If the pair is arranged in a Helmholtz configuration, one may toggle between a uniform field and a field gradient simply by switching the direction of current flow through one of the coils. The field intensity may be adjusted via the computer control system and current driver electronics. The MOT requires approximately 3 amps of current to produce a field gradient of 30 G/cm, whereas studying feshbach resonances requires approximately 25 amps to produce a 1000 G uniform magnetic field.

2.1. Theory

The fields are produced by running electric current through a coil of copper wire loops. The field produced by a circular current loop at an arbitrary coordinate is derived by using the Biot-Savart law:

$$dB = \frac{\mu_o I}{4\pi} \frac{d\vec{l} \times \vec{r}}{r^2}$$

Applied to the current loop and converted to cylindrical coordinates yields [2]:

$$B_z = \frac{\mu I}{2\pi} \frac{1}{\sqrt{(R+\rho)^2 + (z-D)^2}} \left[K(k^2) + \frac{R^2 - \rho^2 - (z-D)^2}{(R-\rho)^2 + (z-D)^2} E(k^2) \right],$$

$$B_\rho = \frac{\mu I}{2\pi} \frac{1}{\rho} \frac{z-D}{\sqrt{(R+\rho)^2 + (z-D)^2}} \left[-K(k^2) + \frac{R^2 + \rho^2 - (z-D)^2}{(R-\rho)^2 + (z-D)^2} E(k^2) \right],$$

where

$$k^2 = \frac{4R\rho}{(R+\rho)^2 + (z-D)^2}.$$

B_z = field along z-axis

B_p = field along radial axis

ρ = radial coordinate

z = vertical coordinate

R = Coil Radius

D = Coil distance from trap center

K = Complete elliptic integral, 1st type

E = Complete elliptic integral, 2nd type

The above equations give a field vector in cylindrical coordinates because there is complete field symmetry about the z-axis, as the coil is assumed to be centered on the z-axis and translated a distance D above the origin. Using superposition, the results from two separate coils can be summed to find the overall field produced by a pair of coils; one above the trap center and one below the trap center.

A power series expansion reveals an optimal geometric spacing of the coil pair, called the Helmholtz configuration. When the coil separation is equal to the coil radius, cancellation results in a linear term but no second or third order terms, making the field linear to third order. [2]

$$B_z = \mu I \frac{8}{5\sqrt{5}R} + \dots ,$$
$$B_\rho = 0 + \dots .$$

Note there is no radial component to the field. The gradient for the MOT is produced when the current in one coil is reversed. This is called the anti-Helmholtz configuration. In this case the field at trap center is zero because the effects from one coil cancel the other, and as you travel toward one coil it becomes more and more dominated by its field. [2]

$$\frac{dB_z}{dz} = \mu I \frac{48}{25\sqrt{5}R^2} = 2\frac{dB_\rho}{d\rho}.$$

It is also important to note that if the field on the x-y plane increases with ρ, then the field along z must decease with z. This is a consequence of Maxwell's equation for magnetic field, which states:

$$\Delta \cdot \vec{B} = o$$
$$\frac{dB_x}{dx} + \frac{dB_y}{dy} + \frac{dB_z}{dz} = 0$$

In our case we have cylindrical symmetry, meaning $B_x = B_y = B_\rho$, so

$$\frac{dB_z}{dz} = -2\frac{dB_\rho}{d\rho}$$

Therefore the trapping potential in the z direction is exactly twice as steep in the z-direction as in any radial direction.

2.2. **MATLAB Coil Simulation**

In order to run through design iterations in an efficient manner, the magnetic field equations were implemented in MATLAB such that a vector field would be calculated for each point in a 3D array representing spatial locations.

A GUI with the various free parameters of the coil design was created for easy changes to coil design. The GUI retrieved all the parameters from edit fields, and delivered them to another function which calculated the values for the magnetic field at all the points within the desired size range and proceeded to call the various MATLAB plotting functions.

Note, however, the function cannot simply apply the field equations once for each spatial location. The finite size of the coil windings must be taken into account by summing the effects from each winding.

The field could then be visualized in several types of 3D plots including color-coded slices through the origin indicating field strength on that plane and color-coded contour plots of field strength on a plane through the origin. These plots are useful for estimating the flatness of the field within the relevant trapping location. For the study of feshbach resonances, the uniform field from the Helmholtz configuration must not vary more than 1 ppm over a region roughly 400μm across. For example, if B_o = 1000G, the field over that region cannot vary more than 1mG in any direction. This was a factor in the coil design because to reach this level of uniformity, the coils must be relatively close to satisfying the Helmholtz configuration. Figure 5 shows a contour plot produced from MATLAB simulations of a Helmholtz pair and an anti-Helmholtz pair of inner radius 5cm and spaced a distance of 5.2 cm apart. These plots confirm the field is well within the flatness constraint.

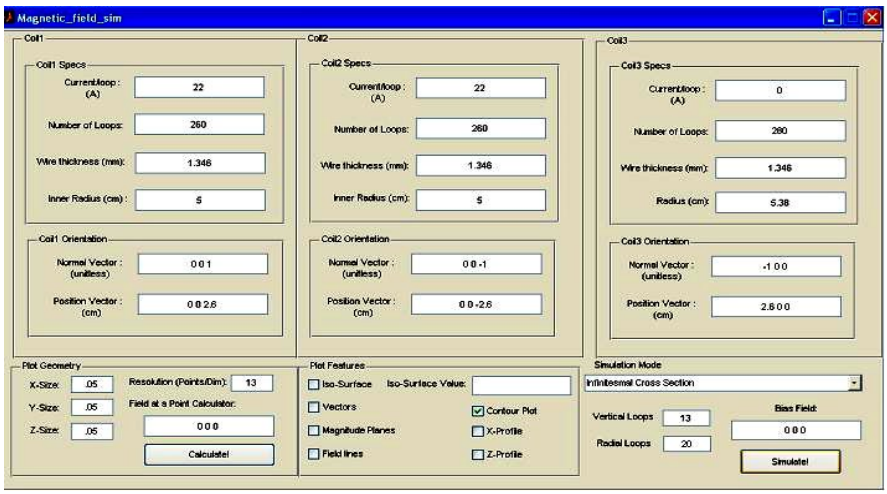

Figure 6: The GUI created in MATLAB for the Magnetic Field Simulations. One can choose the cross-sectional shape of the coil (or a single infinitesimally thin wire) as well as other parameters such as position, orientation, wire thickness, number of loops, and coil radius.

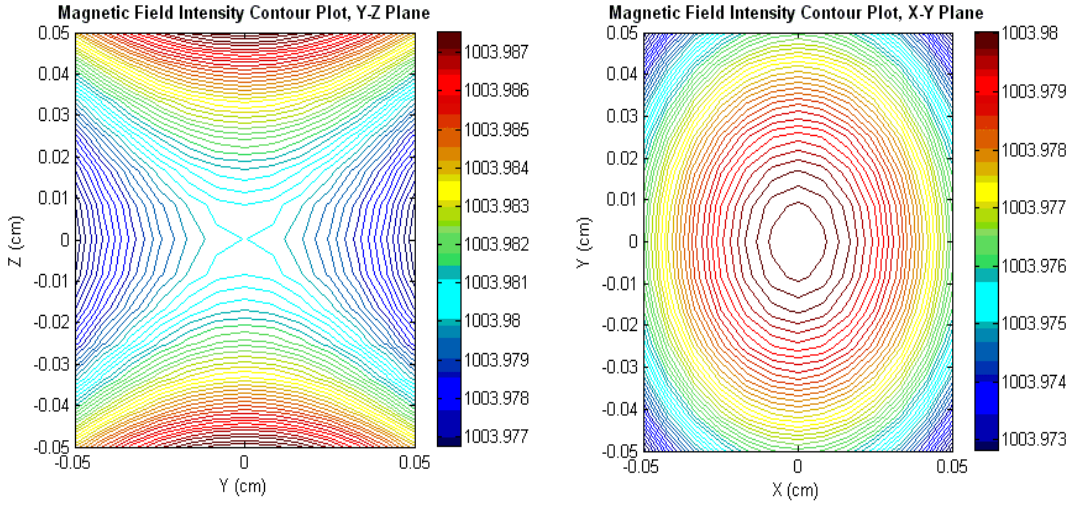

Figure 7: (left)The y-z plane of the uniform field exhibits a saddle point. (right) The x-y plane is symmetric, and has a maximum at the origin.

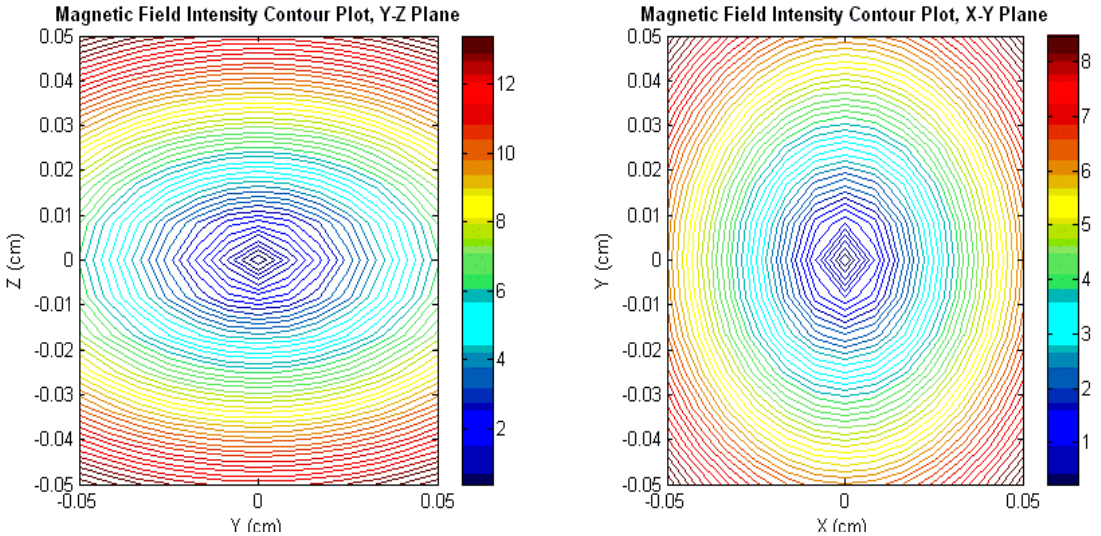

Figure 8: (left) The y-z plane of the gradient field. Note the stronger z gradient. (right) The x-y plane has a symmetric gradient.

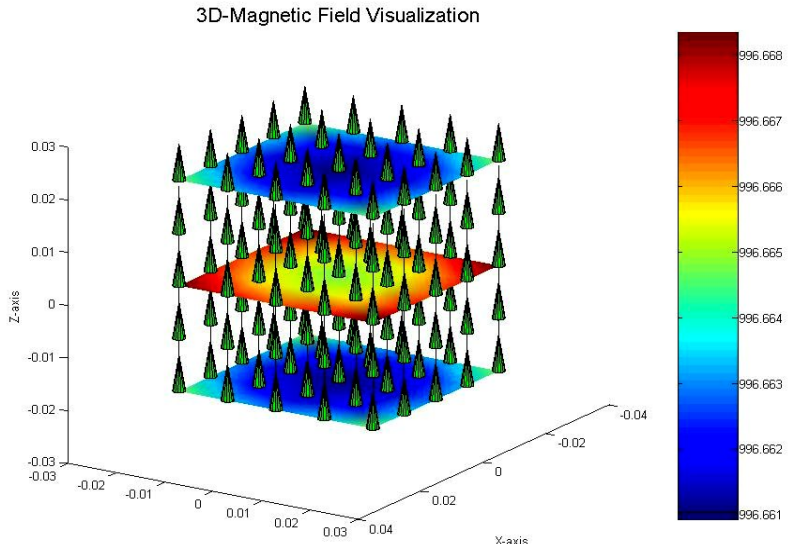

Figure 9: A 3D Visualization of the magnetic field created by a Helmholtz pair. These were not used for quantitative purposes.

2.2.1. Geometry, Power, and Cooling

The MATLAB GUI calculated not only field properties, but also other considerations such as coil resistance, inductance, wire length, power dissipated, and the amount of water necessary for cooling. The size and shape of the coil must meet the magnetic field requirements, but it also must be possible and practical. The size and shape of the vacuum cell presents some limitations. As shown in the introduction and section 4, the quartz vacuum cell is mostly spherical, but has viewing windows and 'arms' from which to load atoms and attach the UHV pump. The atom-loading arm protrudes at about a 43º angle from the UHV arm, leaving a triangle-shaped region where the lower coil may pass through and around the rest of the chamber. It was necessary to make the coil radius large enough to avoid contact with the lower arm, but small enough not to contact the 1.33" conflat mini UHV flange on the end of the horizontal arm.

Within the absolute size restraints imposed by the chamber, there was a tradeoff between having a larger, farther coil with better field uniformity and optical access, and having a smaller, closer coil using less current and therefore less power. Because power is proportional to I^2 and I is linearly proportional to the coil separation, moving them farther away had a large impact on the power requirements.

After some experimenting it was clear that the average vertical separation was optimal at 5.2cm, where they would be close to the trap center and would also have enough room for

0.1” of PVC housing plus a 0.1” gap to allow for water flow. At this separation, a coil of total height 1.75 cm could be placed around the cell. It was also found that the ratio of field strength to coil power could be increased by making more windings extend out radially, while keeping the field uniformity well within tolerance. The final design consisted of a rectangular cross section with 13 vertical windings and 20 radial windings.

The following equations were added to the MATLAB simulation so it could output them to the screen every time the simulation was run. Clockwise from the upper left we have: length of wire, resistance, power, water flow rate, and inductance:

$$l = \pi N(R_{Inner} + R_{outer}) = 2\pi N\overline{R} \qquad R = \frac{\rho l}{A} \qquad P = I^2 R$$

$$f = \frac{P}{c\Delta T\rho} \qquad L = N^2 \overline{R}\mu\left[\ln\left(\frac{8\overline{R}}{a}\right) - 2\right]$$

The inductance calculation is a rough estimate used to calculate the possible switch-off time for the coils while running their full current. Section 3 contains more detail on current driver electronics, however in general it is desirable to have a lower inductance for a shorter switch-off time.

2.3 PVC Housings and water flow

Following a design similar to that used by Todd Meyrath in Texas[2], the coils are to be water cooled with water flowing directly though the windings. The water enters on the bottom, flows up through the windings, then circumferentially around to the return pipe on the other side. The kapton-coated magnet wire offers thin, waterproof insulation well suited for this purpose. Assuming a 2º C change in temperature in the pumped water, the water flow rate is found by dividing the power dissipated in the coils by the energy absorbing capacity of the water. For these coils run at 25 amps, 6 L/min of water flow is required for

Figure 10: Supplemental IRONCAD drawing of the magnetic coil housing. The top piece (‘hat’) is fit over the coil and seals to the base piece, on which the coils are wound. Water and electrical connections are made on the bottom of the base piece.

a 2K temperature change.

PVC plastic was the material chosen for housing for several reasons. First, PVC is very machinable meaning it is not difficult to remove large amounts of material on a mill or lathe. This was done so as to construct the housings from as few pieces as possible, in order to increase rigidity and decrease the risk of a leak at a joint. Second, it is fairly rigid, yet still heat weldable because it is a thermoplastic. It also behaves very well under moist conditions (PVC is the material used in household plumbing pipes). Lastly, it is a non-magnetic material that will not carry eddy currents due to a changing magnetic field. The coil housing face opposite the supply and return water connections is built with a small gap to allow for water flow. There are also layers of 1/16 inch phenolic spacer rods interspersed among the coil windings to separate them enough to allow for water flow between them. Phenolic rods were chosen as material for the inter-winding spacers because they offer exceptional dimensional stability and are a rigid thermoset plastic. This is important in controlling any thermal expansion that arises from imperfect cooling.

The water flow is provided by a Neslabs HX-150 recirculating laboratory water chiller with a buffer tank and a 4.5 kW cooling capacity. The coils will be run in parallel for water flow, but in series for electrical current.

Figures 11 and 12: Photographs of the prototype coil. (left) The complete and sealed prototype coil with brass compression fit elbows connecting to polyethylene tubing. (right) The separating joint of the water and electrical supplies is shown.

The water and electrical connections are made through the same 0.5 inch holes in the bottom of the base. Magnet wire passes from the coil out through custom PVC tubes, into brass elbows connected to the polyethylene tubing and out through a hole drilled in the copper tube shown in figure 12. The hole was soldered then coated in epoxy to ensure a

good seal. The wire travels a short distance outward to a copper bracket in which it is clamped and soldered. At this point the current continues on back to the power supply, separate from the cooling system.

2.4. Prototype Construction

One complete coil prototype was built to 'work out the bugs' of the construction process. Both the housings and the coils themselves were made in the student machine shop. Stock PVC plastic was ordered from www.johnstonplastics.com in the form of a large 1.5 inch thick slab. Each piece was roughed out with the band saw from an 8x8 inch square. Next, the fly cutter was used on the milling machine to make the 3.94 inch hole in the center of the roughed plastic. This large hole could then be used as a grip for the chuck jaws on the lathe; on which the rest of the machining was done. When the water enters through the pipe, it must have a means of traveling radially to reach all the windings. The mill was used to create water flow grooves 0.03 inches deep on the face of the base piece. The grooves run under the windings and don't affect their shape. After the housing was finished, the coils could be wound. The base piece was mounted on a rotate-able milling chuck and slack wire fed through the entrance hole and secured in place. The spool of wire was mounted at the same height as the base piece, but on a vertical rod held in a clamp so it could rotate freely as more wire was needed. One layer was wound at a time, stopping several times along the way to apply liberal amounts of super glue. Two layers were completed, and then a spacer layer was installed. The spacer rods were also super glued in place, but oriented perpendicular to the direction of winding. They also acted as supports on which to wind the next layer. After the first spacer layer, one spacer layer was installed for every three layers of wire. Once all 20 layers were complete, slack wire was measured out and then cut from the spool. The slack was fed through the exit hole in the base piece.

Figure 13: The prototype coil during construction.

With all components complete, the coil could be sealed inside the housing. Acetone was used as a primer for Oatey brand PVC cement to make the seal. Cement was applied all around both edges where the base piece contacts the hat. Because the bottom of the housing is flat, it could be rested in place on a table without any clamps while the cement set up.

2.5. Prototype Testing Results

Before the design complete, it must be tested to at least the maximum reasonable stresses it will experience during experiment. Optimally, upwards of 50 amps would have been pushed through the coils with water cooling at its maximum without leakage. Unfortunately, the PVC cementing did not hold up to the pressure of the recirculating pump, and began leaking immediately. The leaky spots were patched up with more cement, which helped considerably but they still dripped continuously. As a result of the poor connections, some modifications were made to the housing design to increase the surface area of cement contact. The machine shop is currently queued up to produce this new design. As done by Meyrath in Texas, it is likely the future coils will be both cemented and welded shut to be sure of the seal.

The inductance of the coils was measured and compared to the predicted theoretical value from the MATLAB simulation. Inductance was measured by constructing a resonant LRC circuit on a breadboard. The test was complicated by the fact that the coil not only has resistance and inductance, but also a small amount of capacitance, whose value is not known. The coil acts as a resistor in series with an inductor and capacitor in parallel because current being pushed through always sees resistance and after a long time the current continues to flow; which it would not if the capacitor was also in series. So, to find the resonant frequency the imaginary portion of the dynamic impedance of the circuit was set equal to zero:

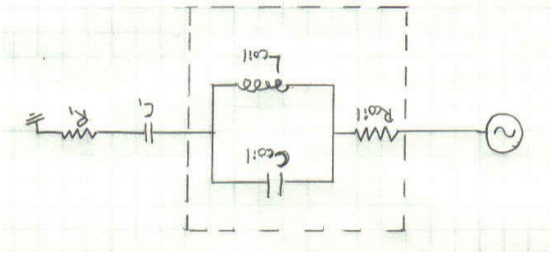

Figure 14: The circuit used to test the coil inductance. Components within the dashed box are part of the coil.

$$\frac{1}{\frac{1}{\omega L} - \omega C_{coil}} - \frac{1}{\omega C_1} = 0$$

$$\omega = \sqrt{\frac{1}{L_{coil}\left(C_1 + C_{coil}\right)}}$$

Several values of C_1 were used and the resonant frequency was found in each case. The datapoints were then plotted and fitted to the above equation for the parameters L and C. The value of inductance found matches well with the estimated value—taking into account the estimation was very rough. The Mathematica file containing the data and fitting parameters is attached as Appendix II.

3.0 A SELF-STABILIZING CURRENT SOURCE

The current running through the coils is to be controlled by a circuit board very similar to that used by the laser diodes for their current supplies. The board is a versatile circuit which takes either a manual input to a potentiometer knob and/or an analog input from a computer to control the amount of current run through a device. Note that for the study of feshbach resonances, it has yet to be determined if the stability of the current model is adequate. Optically the stability would be within 1 ppm, and other techniques are being explored to solve this issue.

3.1. PID Controller

The input is used as a reference voltage to compare against a current-dependant voltage coming from either a 4-point sense resistor or a Hall-effect probe. The current-dependant voltage is amplified by an INA128 instrumentation amplifier, and then sent to an AD820AN operational amplifier with both differential and integral feedback. The AD820AN output can be sent to any device that can convert voltage to current.
Since the multi-purpose trapping coils are to be used for both a Magneto-Optical Trap using barely a few amps and for magnetic trapping using up to 30 amps, two different output stages are being planned for use. The low current output stage would receive the AD820AN signal as input to a few buffer amplifiers run in parallel. The buffers output a current that is directly proportional to the input voltage, and can be stacked in parallel to output a higher current than a single unit can provide. The high current output stage is likely to be made from power MOSFETs. The MOSFETs will control the current from an external high current power supply by being put in series with the coil pair.

3.2. Switching, Optical Isolation, and Shut-Off

The circuit allows the current in the second coil to be reversed in order to toggle between a quadrupole field and a uniform field. As is visible in the schematic switching diagram of figure 14, there will be several points in the circuit where MOSFETs require reference voltages in relation to their local ground. The local grounds will depend on the amount of current flowing through the coils at any point in time because the coils have a small amount of resistance. This poses a problem when the reference voltage comes from an earth grounded current controller. One solution is to separate the coils, MOSFETs, and power supply from the rest of the circuits via optical isolation. There are commercially available optical isolators which have separate grounds on either side, and the through connection is made by having an LED send light to a photodiode. For example, if the input side has a 10V earth grounded signal and the right side has a floating local ground, the output will equal the local ground voltage plus 10V. So no matter what the current is through the coils, the MOSFETs will receive the correct reference voltage. An additional benefit of the isolators is that of protection from voltage spikes during coil shut-off. The voltage across an inductor is:

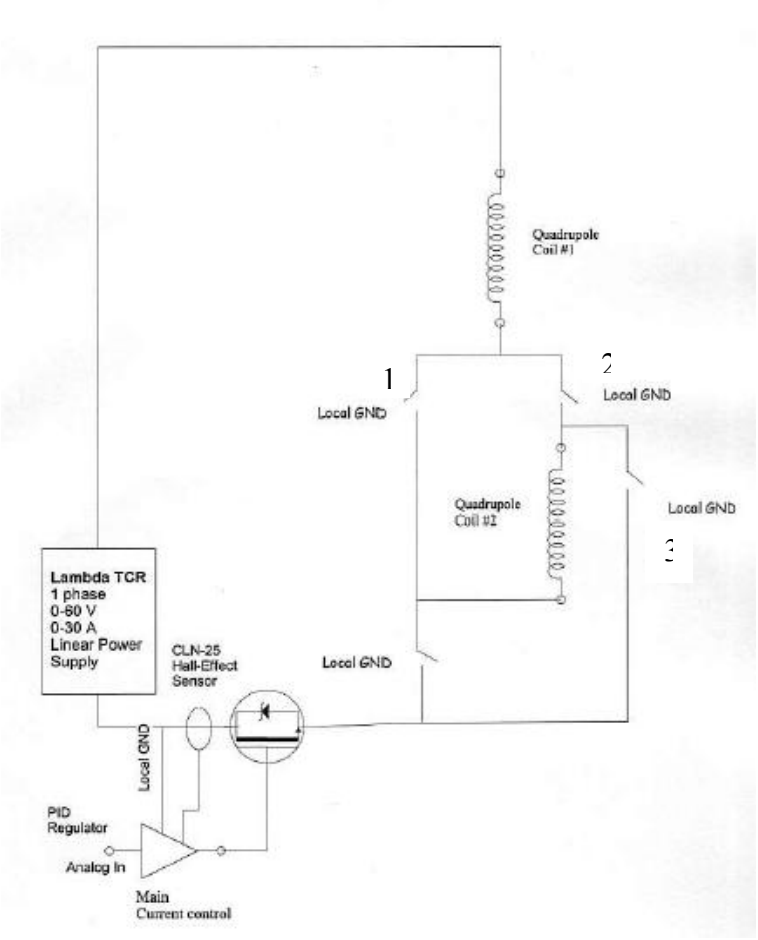

Figure 14: The schematic switching diagram for the multi-purpose trapping coils. The current direction in the second coil may be toggled by closing either switches 1 and 3, or 2 and 4.

$$V_L = L\frac{di}{dt}$$

So if the shut-off is quick, then V_L is large. Computers and other valuable equipment are

connected in some way with the coils, and the isolators are a good precaution against such disaster.

In a normal inductive circuit, V_L will be an exponential decay if the power source is switched off. Although initially rapid, an exponential decay can still have a significant amount of current flowing after a given time lapse. For cold atom experiments, it is generally desirable to have the current completely turn off when the supply is cut. It is not shown in figure 14, but it is possible to 'clamp' the value of V_L at a constant value by putting Zener diodes in parallel with the coils. The Zeners have a reverse breakdown voltage that will remain essentially unchanged no matter what the current is. This makes the current decay linear, and ensures a total shut off of the magnetic field.

4.0 OTHER PROJECTS

In addition to the making the first coil prototype, a second coil housing was machined as well as security keypad boxes for the lab's homebuilt system. The second coil housing is identical to the first, and will possibly be used for further testing of the design, as the testing process is potentially catastrophic.

The lab's security system will use a simple two layer circuit to encode signals from a small LCD display screen and commercially made keypad. The circuits were designed by Tao Kong, a graduate student at QDG lab. They were etched using photolithography right in the lab. Overheads of the circuit layout were printed, and then laid out on a board coated with a chemical photoresistive coating. They were exposed to ten minutes of bright fluorescent light on each side, and soaked in a developer solution. Next, they are rinsed with water and transferred to a heated bath of KOH chemical etchant. The circuits were removed from this heated bath when all the photoresist was visibly etched away, and the circuit looked complete. Testing with the keypads and LCD screens indicated flawless circuitry.

4.1. Laser Diode Response Analysis

The MOT master laser diode is constructed but still under testing; as such several kinds of data were taken to acquire as much information as possible about its response to various stimuli. Both the laser cavity length and diffraction grating angle are controlled via piezoelectric crystals which are driven by special servo boxes made by the physics

electronics shop. The laser's response to driving each of these crystals was recorded by a photodiode. The laser frequency was centered upon the saturated absorption feature of ^{87}Rb, and modulated one at a time by each of the crystals. Scope traces were downloaded in Microsoft Excel format through a GPIB cable in the back of the scope. The data for the driving signal and laser response were taken in raw format into MATLAB and curve fitted to a sine functions with the parameters phase, frequency, and amplitude. The resulting functions were plotted and compared in order to determine any resonances. The piezos were modulated at frequencies from 100Hz up to 1100Hz. The source of the various peaks is still unknown, and is under investigation.

Another dataset was taken to determine the laser's susceptibility to physical vibrations. A couple 'informal' taps of the screwdriver on the optics table were recorded in the photodiode. The Fast Fourier Transform was analyzed to identify the laser's susceptibility to physical disturbances, and to make efforts to dampen those specific frequencies. Three taps were recorded: one 'Lo', one 'Med', and one 'High. The profiles shown in figure 16 are slightly different, indicating the difference in energy required to excite certain modes.

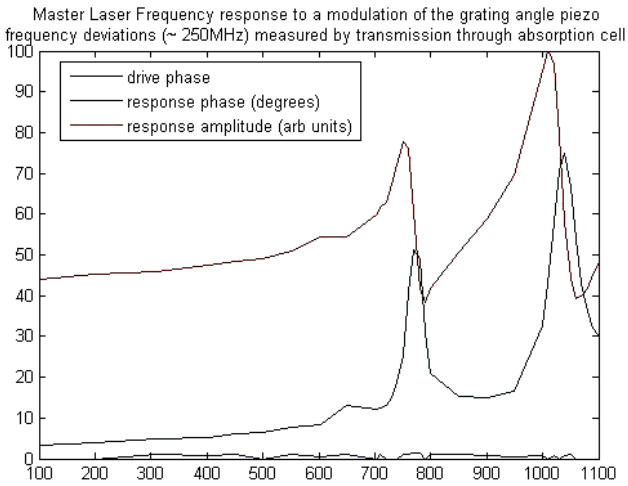

Figure 15: The Master laser frequency response to a diffraction grating-angle piezoelectric crystal modulation.

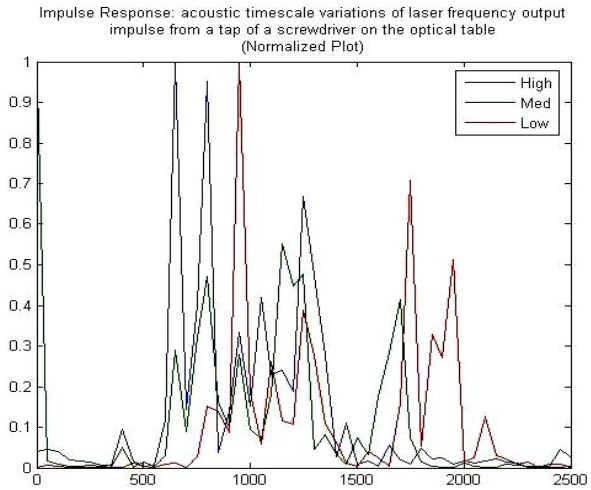

Figure 16: The Master Laser response to physical vibrations. Amplitude corresponds to frequency variation of the laser.

5.0 CONCLUSION/RECOMMENDATIONS

All the aspects of the magnetic coil have been designed and construction has been set in motion. The physics machine shop is queued to build the coil housings to accurate specifications. What remains to be done once the housings are complete is to physically wind the two coils, which is somewhat of a tedious process, but each one may be completed with approximately 2 days of solid work. I have volunteered to build them in my spare time this summer, if any exists.

Judging from the results of the prototype, it is my recommendation that the new coils are welded together using a plastic welding heat gun and PVC solder rod to make certain a solid connection is made between the two pieces of the housing. If the coils are to be used beyond specification during a later experiment, one may desire the most solid plastic connection as possible. After all of the above is complete, the coils may be stress tested to currents upwards of 50 amps and to the maximum water flow rates possible with the Neslabs HX-150 chiller.

With a set of working, switch able coils, the lab may proceed with the remaining tasks required to get a MOT up and running, including but not limited to:

- Slave lasers and Broad-Area-Laser amplification system
- A second master laser
- UHV system running
- Lithium and Rubidium sources secured in UHV chamber

Further in the future, Ioffe-Pritchard or TOP style magnetic trap designs may be implemented. The magnetic field from a set of pure quadrupole coils cannot be used alone for magnetic trapping due to the zero point in the trap center. Both the above designs avoid this flaw by adding more coils, but in much different ways. Both of these designs will also require earth field coils to counteract the earth's own weak magnetic field. These are coils of much larger diameter but of fewer windings and less current. They will likely be adapted to the geometry of the experimental setup, and therefore designed and built in a later term, closer to the completion of the magnetic trap.

6.0 REFERENCES

[1] Cable, Alex, et al. "Trapping of Neutral Sodium Atoms with Radiation Pressure." Physical Review Letters 59 (1987): 2631-2635.

[2] Meyrath, Todd. 15 Nov. 2001. Electromagnet Design for Cold Atom Experiments.

[3] Metcalf, Harold J. Laser Cooling and Trapping. New York: Springer, 1999. 156-162.

[4] Pethick, C. J., and H. Smith. Bose-Einstein Condenstation in Dilute Gases. Cambridge: Cambridge UP, 2002. 79.

7.0 APPENDIX I: SAMPLE MATLAB CODE

```
%Function that calls 'B_field_loop' many many times to find the result of
%having a finite sized coil with N loops.
%NOTE: It is required that Coil 1 be centered on the z-axis, parallel to
%and ABOVE the x-y plane; Coil 2 be centered on the z-axis, parallel
%to and BELOW the x-y plane; and Coil 3 be centered on the x-axis, parallel
%to and POSITIVE of the y-z plane.


function sum = sum_fields(handles, Summing_Point)

mu = (0.4*pi);      %Mu is being used in the form for mixed units: Guass,
cm, Amps

%Field_Point = [0 0 0]; %If no value is given, use the zero vector as a default
point to display
                        %the field at.

n1 = str2num(get(handles.Normal1_edit, 'String'));
r1 = str2num(get(handles.Position1_edit, 'String'));
R1 = str2num(get(handles.Radius1_edit, 'String'));
I1 = str2num(get(handles.Current1_edit, 'String'));
n2 = str2num(get(handles.Normal2_edit, 'String'));
r2 = str2num(get(handles.Position2_edit, 'String'));
R2 = str2num(get(handles.Radius2_edit, 'String'));
I2 = str2num(get(handles.Current2_edit, 'String'));
n3 = str2num(get(handles.Normal3_edit, 'String'));
r3 = str2num(get(handles.Position3_edit, 'String'));
R3 = str2num(get(handles.Radius3_edit, 'String'));
I3 = str2num(get(handles.Current3_edit, 'String'));
%Field_Point = str2num(get(handles.at_a_Point, 'String'));
Num_Loops1 = str2num(get(handles.Loop1_edit, 'String'));
Num_Loops2 = str2num(get(handles.Loop2_edit, 'String'));
Num_Loops3 = str2num(get(handles.Loop3_edit, 'String'));
Thick1 = str2num(get(handles.Wire1_edit, 'String'))/10;   %Convert to cm
Thick2 = str2num(get(handles.Wire2_edit, 'String'))/10;   %Convert to cm
Thick3 = str2num(get(handles.Wire3_edit, 'String'))/10;
NLoops_Radial = str2num(get(handles.Radial_Loops, 'String'));
NLoops_Vertical = str2num(get(handles.Vertical_Loops, 'String'));


Side_length = floor(sqrt(Num_Loops1));

%Spacer Thickness, converted to cm
spacer = (1/16)*2.54;

summed_Coil1 = [0 0 0]';
summed_Coil2 = [0 0 0]';
summed_Coil3 = [0 0 0]';

%create temp inner radii
R1_temp = R1;
R2_temp = R2;
R3_temp = R3;

%set temps to bottom
```

```
r1_temp = r1 - [0 0 1].*0.5*NLoops_Vertical*Thick1;
r2_temp = r2 + [0 0 1].*0.5*NLoops_Vertical*Thick2;
r3_temp = r3 - [1 0 0].*0.5*NLoops_Vertical*Thick3;

for i = 1:NLoops_Radial
    for j = 1:NLoops_Vertical
        summed_Coil1 = summed_Coil1 + (mu/(2*pi))*(I1*B_field_loop(n1,
Summing_Point,r1_temp, R1_temp));
        summed_Coil2 = summed_Coil2 + (mu/(2*pi))*(I2*B_field_loop(n2,
Summing_Point,r2_temp, R2_temp));
        summed_Coil3 = summed_Coil3 + (mu/(2*pi))*(I3*B_field_loop(n3,
Summing_Point,r3_temp, R3_temp));
        r1_temp(3) = r1_temp(3) + Thick1;
        r2_temp(3) = r2_temp(3) - Thick2;
        r3_temp(1) = r3_temp(1) + Thick3;
    end
r1_temp = r1 - [0 0 1].*0.5*NLoops_Vertical*Thick1;     %reset to bottom
r2_temp = r2 + [0 0 1].*0.5*NLoops_Vertical*Thick2;
r3_temp = r3 - [1 0 0].*0.5*NLoops_Vertical*Thick3;

%increase radius by Thick1, and add spacer every 3 layers
    R1_temp = R1_temp + Thick1;
    R2_temp = R2_temp + Thick2;
    R3_temp = R3_temp + Thick3;
    if ~(mod(i,3))
            R1_temp = R1_temp + spacer;
            R2_temp = R2_temp + spacer;
            R3_temp = R3_temp + spacer;

    end

end
summed_field = summed_Coil1 + summed_Coil2 + summed_Coil3;

%display('Field at the point');
%disp(Summing_Point');
%disp('Is equal to:');
%disp(summed_field);
sum = [summed_field, summed_Coil1, summed_Coil2, summed_Coil3];
```

8.0 APPENDIX II: MATHEMATICA ANALYSIS OF COIL INDUCTANCE

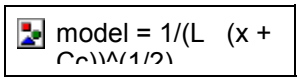

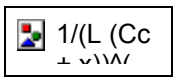

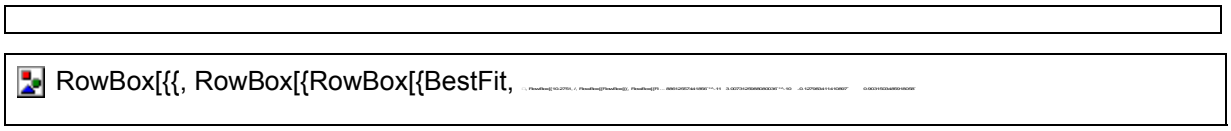

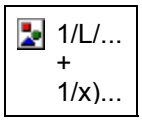

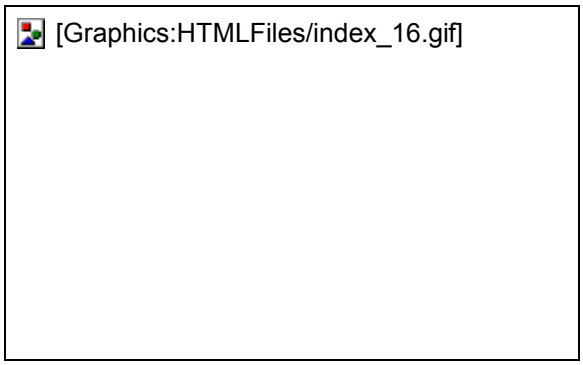

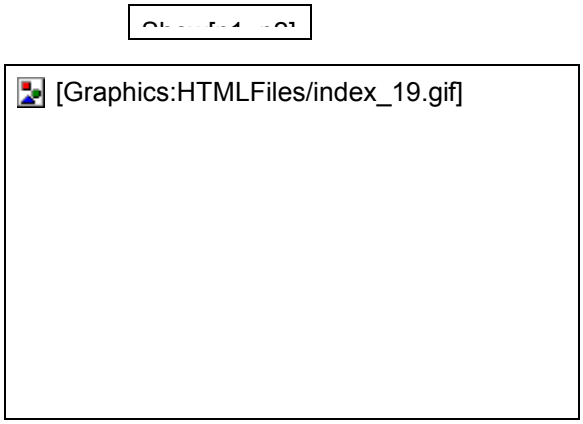

Created by *Mathematica* (May 4, 2005)

The fitted value for the coil inductance is 9.47 mH, which agrees nicely with the predicted value of 7.4 mH. The prediction is a very rough estimate using average coil radius and does not take into account spacer layers and many other factors. The negative value for coil capacitance is likely explained by the miniscule real value of the coil capacitance combined with the uncertainty of the commercial capacitors C_1. My thanks to Aviv Keshet for helping me with this Mathematica analysis.